Planta (2010) 231:461–474
DOI 10.1007/s00425-009-1067-3

ORIGINAL ARTICLE

Importance of ROS and antioxidant system during the beneficial interactions of mitochondrial metabolism with photosynthetic carbon assimilation

Challabathula Dinakar · Vishwakarma Abhaypratap · Srinivasa Rao Yearla · Agepati S. Raghavendra · Kollipara Padmasree

Received: 30 July 2009 / Accepted: 6 November 2009 / Published online: 27 November 2009

Abstract The present study suggests the importance of reactive oxygen species (ROS) and antioxidant metabolites as biochemical signals during the beneficial interactions of mitochondrial metabolism with photosynthetic carbon assimilation at saturating light and optimal CO_2. Changes in steady-state photosynthesis of pea mesophyll protoplasts monitored in the presence of antimycin A [AA, inhibitor of cytochrome oxidase (COX) pathway] and salicylhydroxamic acid [SHAM, inhibitor of alternative oxidase (AOX) pathway] were correlated with total cellular ROS and its scavenging system. Along with superoxide dismutase (SOD) and catalase (CAT), responses of enzymatic components—ascorbate peroxidase (APX), monodehydroascorbate reductase (MDAR), glutathione reductase (GR) and non-enzymatic redox components of ascorbate–glutathione (Asc–GSH) cycle, which play a significant role in scavenging cellular ROS, were examined in the presence of mitochondrial inhibitors. Both AA and SHAM caused marked reduction in photosynthetic carbon assimilation with concomitant rise in total cellular ROS. Restriction of electron transport through COX or AOX pathway had differential effect on ROS generating (SOD), ROS scavenging (CAT and APX) and antioxidant (Asc and GSH) regenerating (MDAR and GR) enzymes. Further, restriction of mitochondrial electron transport decreased redox ratios of both Asc and GSH. However, while decrease in redox ratio of Asc was more prominent in the presence of SHAM in light compared with dark, decrease in redox ratio of GSH was similar in both dark and light. These results suggest that the maintenance of cellular ROS at optimal levels is a prerequisite to sustain high photosynthetic rates which in turn is regulated by respiratory capacities of COX and AOX pathways.

Keywords Antioxidants · Alternative oxidase · Cytochrome oxidase · Pea · Photosynthesis · Reactive oxygen species

Abbreviations

AA	Antimycin A
AOX	Alternative oxidase
APX	Ascorbate peroxidase
Asc	Ascorbate reduced
CAT	Catalase
COX	Cytochrome oxidase
DHA	Dehydroascorbate
GR	Glutathione reductase
GSH	Glutathione (reduced)
GSSG	Glutathione (oxidized)
MDAR	Monodehydroascorbate reductase
ROS	Reactive oxygen species
SOD	Superoxide dismutase

Introduction

In photosynthetic tissues, mitochondria play an important role in benefiting chloroplastic photosynthesis by backing up carbon assimilation through cytochrome oxidase (COX)

Electronic supplementary material The online version of this article (doi:10.1007/s00425-009-1067-3) contains supplementary material, which is available to authorized users.

Ch. Dinakar · V. Abhaypratap · S. R. Yearla · A. S. Raghavendra · K. Padmasree (✉)
Department of Plant Sciences, School of Life Sciences, University of Hyderabad, Hyderabad 500046, India
e-mail: kpssl@uohyd.ernet.in

and alternative oxidase (AOX) pathways by different mechanisms (Padmasree and Raghavendra 1999a, b, 2001a, b). The two terminal oxidases, COX and AOX, associated with these two pathways are involved in reducing molecular oxygen to H_2O. The energy released during the electron transport through COX pathway is coupled to the synthesis of ATP. This function of COX pathway is known to benefit sucrose biosynthesis (Padmasree and Raghavendra 1999b). On the other hand, though the passage of electrons from ubiquinone to AOX pathway does not generate any ATP, it has a significant function in preventing over-reduction of not only respiratory complexes but also electron transport carriers of chloroplasts (Yoshida et al. 2006, 2007; Noguchi and Yoshida 2008).

The existence and operation of respiration in light were debated until past two decades (Graham 1980). However, the significance of mitochondrial bioenergetic metabolism in benefiting photosynthetic carbon assimilation was revealed in several reviews (Raghavendra et al. 1994; Krömer 1995; Hoefnagel et al. 1998; Gardeström et al. 2002; Padmasree et al. 2002; Raghavendra and Padmasree 2003; Noctor et al. 2007; Noguchi and Yoshida 2008; Nunes-Nesi et al. 2008). Usage of specific metabolic inhibitors and generation of specific mutants/transgenic plants which either under-express or over-express a specific key component related to respiratory process clearly established the importance of bioenergetic oxidative metabolism over TCA cycle in optimizing photosynthesis (Krömer et al. 1993; Padmasree and Raghavendra 1999a; Carrari et al. 2003; Dutilleul et al. 2003; Fiorani et al. 2005; Nunes-Nesi et al. 2005, 2008; Yoshida et al. 2006, 2007). The different components of bioenergetic metabolism of mitochondria, which include the activities of oxidative phosphorylation, rotenone-sensitive complex I, rotenone-insensitive external and internal NAD(P)H dehydrogenases, antimycin A (AA)-sensitive COX pathway, salicylhydroxamic acid (SHAM)-sensitive AOX pathway and reactive oxygen species (ROS) activated uncoupling proteins (UCP) were found to be essential for efficient functioning of chloroplastic photosynthesis (Krömer et al. 1988; Igamberdiev et al. 1998; Padmasree and Raghavendra 1999a; Møller 2001; Dutilleul et al. 2003; Sweetlove et al. 2006; Yoshida et al. 2006, 2007).

Generation of ROS from redox reactions of chloroplasts and mitochondria has been identified as an inevitable process of aerobic metabolism (Møller 2001; Apel and Hirt 2004; Noctor 2006; Møller et al. 2007). Four major types of ROS, singlet oxygen ($^1O_2$), superoxide (O_2^-), hydrogen peroxide (H_2O_2) and hydroxyl radicals (OH^-), are produced in green tissues during active photosynthesis. In chloroplasts, PSII and PSI are the major sites for the production of singlet oxygen and superoxide radicals (Apel and Hirt 2004). In mitochondria, complex I, ubiquinone and complex III of electron transport chain are the major sites for the generation of superoxide radicals (Møller 2001; Navrot et al. 2007). In both these organelles, O_2^- radicals are immediately dismutated to H_2O_2, a less toxic form of ROS, by superoxide dismutase (SOD). H_2O_2 is also formed as a by-product of photorespiration during oxidation of glycolate to glyoxylate in peroxisomes (del Rio et al. 2006). Both O_2^- and H_2O_2 participate in a fenton-type reaction with free Cu and Fe ions available in the cell and generate OH^- radicals.

Traditionally, ROS were considered to be toxic by-products of aerobic metabolism, which were disposed of using antioxidants (Asada 1999; Apel and Hirt 2004; Noctor et al. 2007). However, in recent years, it has become apparent that plants actively produce ROS as signaling molecules to control processes such as growth, cell cycle, programmed cell death, abiotic stress responses, pathogen defense, systemic signaling and development (Mittler et al. 2004; Møller et al. 2007). The intensity, duration and localization of different ROS signals are determined by the interplay between the ROS production and ROS scavenging pathways of the cell. AOX and UCP of the mitochondrial electron transport were suggested to be proactive enzymes for ROS avoidance in plants. The suggested pathways for ROS scavenging along with catalase (CAT) were (a) the water–water cycle, (b) the ascorbate–glutathione (Asc–GSH) cycle and (c) the glutathione peroxidase (GPX) cycle. In all these pathways, SOD acts as the first line of defense converting O_2^- into H_2O_2. H_2O_2 is subsequently detoxified by CAT, ascorbate peroxidase (APX) and GPX. In contrast to CAT, APX and GPX require an ascorbate (Asc) and/or a glutathione (GSH) regenerating cycle, which use electrons from NAD(P)H. The NAD(P)H-dependent pathways of ROS scavenging mechanisms act either by reducing ROS directly or by protecting or regenerating the oxidized proteins (Navrot et al. 2007). Studies with knock out and antisense lines for antioxidant enzymes revealed strong link between the ROS and the processes such as growth, development, biotic and abiotic stress responses. The intra-cellular localization of ROS scavenging antioxidant system has been detected in all the following compartments of the plant cells: chloroplasts (grana and stroma), peroxisomes, mitochondria and cytosol using classical fractionation techniques, enzymatic analysis, GFP chimeric proteins, gene expression and proteomic approaches (Doulis et al. 1997; Chew et al. 2003; Mittler et al. 2004; Sundar et al. 2004; Palma et al. 2006, Navrot et al. 2007).

Direct role of ROS in signal transduction is ensured only if ROS escape destruction by antioxidants or otherwise consumed in a ROS cascade. Thus, the major low molecular weight antioxidants Asc and GSH determine the

specificity of the signal. Along with ROS, Asc and GSH also act as signal-transducing molecules that can either signal independently or further transmit ROS signals. The specific interplay between ROS and the Asc–GSH cycle constituents generated compartment (chloroplastic, mitochondrial, cytosolic and peroxisomal) specific changes in both the absolute concentrations of ROS and antioxidant compounds, and thereby changes in redox ratio of Asc (indicated as Asc/DHA) and GSH (indicated as GSH/GSSG) during *Botrytis cinerea* infection in tomato leaves (Kuzniak and Sklodowska 2005).

The information on the role of redox-related metabolites such as malate (Mal), oxaloacetate (OAA), triose-P and PGA in the biochemical cross-talk between chloroplasts and mitochondria during active photosynthesis is well established (Padmasree and Raghavendra 1999b; Noguchi and Yoshida 2008). AOX was suggested as an essential component in antioxidant defense mechanism for the control of a balanced C/N metabolism (Watanabe et al. 2008). The experiments using transformed *Arabidopsis thaliana* with modified AOX protein indicated that the overall ability of leaves to produce and accumulate ascorbic acid is dependent on the regulation of L-GalLDH activity via the interaction of light and respiratory controls (Bartoli et al. 2006).

The role of ROS and nitric oxide (NO) as signals has been suggested in the biochemical cross-talk between the metabolic compartments: chloroplasts and mitochondria (Raghavendra and Padmasree 2003). Hence, in the present study, an attempt was made to evaluate the importance of ROS and antioxidant system, which includes antioxidant enzymes and metabolites, during the beneficial interactions between chloroplasts and mitochondria to optimize photosynthetic carbon assimilation. The use of mesophyll protoplasts is an excellent model to examine the responses of respiration, photosynthesis, ROS and antioxidant enzymes/metabolites within short period of 10 min duration as they easily permeate exchange of O_2, CO_2 and metabolic inhibitors: AA and SHAM (Padmasree and Raghavendra 1999a; Strodtkötter et al. 2009).

Materials and methods

Plant material

Pea plants (*Pisum sativum* L. cv. Arkel; seeds obtained from Pocha seeds, Pune, India) were grown outdoors under natural photoperiod of approximately 12 h and average daily temperatures of 30°C day/20°C night. The second pair of fully unfolded leaves were picked from 8- to 10-day-old plants and used for isolation of mesophyll protoplasts.

Isolation of mesophyll protoplasts

The mesophyll protoplasts were isolated from leaf strips devoid of lower epidermis by enzymatic digestion with 2% (w/v) Cellulase Onozuka R-10 and 0.2% (w/v) Macerozyme R-10 (Yakult Honsha Co. Ltd., Nishinomiya, Japan), under low light intensities of 50–100 μmol m^{-2} s^{-1}. The protoplasts were collected by filtration through 60 μm nylon filter and purified by centrifugation at 100*g* for 5 min, thrice at 4°C. The protoplasts were finally stored on ice in suspension medium (10 mM Hepes–KOH, pH 7.0, 0.4 M sorbitol, 10 mM $CaCl_2$, 0.5 mM $MgCl_2$) and chlorophyll was estimated (Padmasree and Raghavendra 1999a).

Isolation of chloroplasts from mesophyll protoplasts

The protoplasts were ruptured by passing through a 2 ml disposable syringe fitted with a 22.5 μm nylon filter. The chloroplasts were isolated from broken protoplasts by centrifuging at 250*g* for 2 min. The chloroplast pellet was suspended in a medium containing 50 mM Hepes–KOH, pH 7.6, 0.4 M sorbitol, 0.5 mM $MgCl_2$, 1 mM $MnCl_2$, 10 mM Na_2-EDTA and 0.4% BSA.

Monitoring respiration and photosynthesis

The O_2 uptake (respiration) and evolution (photosynthesis) rates of the mesophyll protoplasts equivalent to 10 μg Chl contained in reaction medium (0.4 M sorbitol, 1 mM $CaCl_2$, 1 mM $MgCl_2$, 10 mM Hepes–KOH, pH 7.5) were monitored polarographically at 25°C using a Clark-type oxygen electrode system, controlled by HansaTech software (King's Lynn, Norfolk, UK). The respiratory rates were measured during the dark period. The rates of photosynthesis were measured for 10 min after a brief dark period (5 min) using a light source (1,000 μmol m^{-2} s^{-1}) provided by a 35 mm slide projector [xenophot (halogen) lamp, 24 V/150 W]. $NaHCO_3$ (1.0 mM) was added to the reaction medium before dark treatment. Oxygen content in the electrode chamber was precalibrated at 25°C with air-saturated water using sodium dithionate. The rates of photosynthesis in isolated chloroplasts were monitored as described elsewhere (Padmasree and Raghavendra 1999a).

Treatment of mesophyll protoplasts or chloroplasts with test compounds

Mitochondrial respiratory inhibitors, AA and SHAM, procured from Sigma (Sigma, St. Louis, MO, USA) were dissolved in ethanol and added to the reaction medium to give the required final concentrations, during the dark

period before the mesophyll protoplasts or chloroplasts were exposed to normal light.

Total respiration, capacities of COX and AOX pathways

Total respiration is the rate of O_2 uptake in the absence of any inhibitors. Once a steady respiratory rate was attained, mitochondrial inhibitors were added directly to the samples in the cuvette to measure the capacities of COX and AOX pathways. As the adenylates determine the flux of electrons through COX pathway, the capacity of COX pathway was determined as the O_2 uptake sensitive to 1 mM KCN in the presence of both 1 μM CCCP (uncoupler) and SHAM (10 mM). The capacity of AOX pathway was determined as the O_2 uptake sensitive to 10 mM SHAM in the presence of 1 mM KCN (Vanlerberghe et al. 2002).

Detection of ROS

Reactive oxygen species levels in mesophyll protoplasts or chloroplasts were measured using a fluorescent dye, 2,7-dichlorofluorescein diacetate (H_2DCF-DA). This non-polar compound is converted to membrane-impermeant polar derivative H_2DCF by cellular esterases and is rapidly oxidized to highly fluorescent DCF by intra-cellular H_2O_2 and other peroxides. Stocks of H_2DCF-DA (1 mM) were made in ethanol and stored in the dark at −80°C. The mesophyll protoplasts or chloroplasts pre-incubated in H_2DCF-DA (1 mM) in dark for 30 min, after a series of brief centrifugation steps of 100*g* were finally resuspended in an aliquot of suspension medium, so as to dilute the concentration of H_2DCF-DA to 5 μM. DCF fluorescence of the mesophyll protoplasts at 0 min and after incubation for 10 min in dark or light (1,000 μmol m^{-2} s^{-1}) in the absence and presence of mitochondrial electron transport inhibitors was measured using Hitachi F-4010 fluorescence spectrophotometer (Chiyoda-ku, Tokyo, Japan) with excitation and emission wavelengths set at 488 and 525 nm, respectively. DCF fluorescence of the chloroplasts was also measured after illumination for 10 min in the presence of AA (0.1 μM) and SHAM (0.5 mM). In some of the experiments, a confocal microscope (TCSSP-2, AOBS 4 channel UV and visible; Leica, Heidelberg, Germany) was used to observe the fluorescence of ROS from mesophyll protoplasts of pea (excitation filter 488 nm, emission 500–550 nm).

Western blotting

Reaction medium containing mesophyll protoplasts equivalent to 10 μg Chl was withdrawn after exposure of protoplasts to light for 10 min in the presence of different concentrations of AA and SHAM. These samples were snap frozen in liquid nitrogen after a brief centrifugation step at 100*g* for <1 min. The frozen-pelleted protoplasts were homogenized in 125 mM Tris–HCl (pH 6.8) containing 5% (w/v) SDS and 1 mM PMSF. The homogenate was centrifuged at 10,000*g* for 10 min and supernatant was collected. To the supernatant, protein estimation was done following the method of Lowry et al. (1951). SDS-PAGE of mesophyll protoplast proteins was performed according to Laemmli (1970) using 14 × 8 cm wide mini gels. In each well, 8 μg protein was loaded. The proteins separated on 12.5% SDS-PAGE were transferred electrophoretically from the gel onto polyvinylidene difluoride (PVDF) membranes (Towbin et al. 1979). The blots were probed with anti-PsbA (anti-D1, 1:2,000) antibodies (Agrisera, Vännäs, Sweden) followed by 1:5,000 dilution of goat anti-rabbit IgG alkaline phosphatase conjugate. Finally, the blot was developed using nitro-blue-tetrazolium chloride and 5-bromo-4-chloro-3-indolyl phosphate as substrates.

Preparation of enzyme extract and assay of antioxidant enzymes

Aliquots (600 μl) of reaction medium containing protoplasts equivalent to 100 μg Chl were withdrawn at 0 min and after incubation for 10 min in dark or light (1,000 μmol m^{-2} s^{-1}) in the absence and presence of AA and SHAM. These samples were snap frozen in liquid nitrogen after a brief centrifugation step at 100*g* for <1 min. Before enzymatic assays, the pelleted protoplasts were homogenized in 50 mM phosphate buffer pH 7.0 containing 1 mM PMSF. The homogenate was centrifuged at 10,000*g* for 10 min and the supernatant was used for the assay of CAT, APX, MDAR and GR. For SOD assay, the pelleted protoplasts were homogenized in 50 mM phosphate buffer pH 7.8 containing 1 mM PMSF. Protein concentration in the enzyme extracts was determined by the method of Lowry et al. (1951) using defatted BSA as a standard.

Superoxide dismutase (SOD, E.C. 1.15.1.1)

Superoxide dismutase activity was determined by the method of Beauchamp and Fridovich (1971). The required cocktail for the estimation of SOD activity was prepared by mixing 27 ml of sodium phosphate buffer (pH 7.8), 1.5 ml of methionine (300 mg ml^{-1}), 1 ml of NBT (14.4 mg 10 ml^{-1}), 0.75 ml of Triton-X 100 and 1.5 ml of 2 mM EDTA. To 1 ml of this cocktail, 10 μl of riboflavin (4.4 mg 100 ml^{-1}) and enzyme extract containing 50 μg of protein were added. The reaction mixture taken in the cuvette was illuminated for 8 min using three comptalaux bulbs (100 W, Philips India Ltd.). The

temperature was maintained at 25°C using a water bath. A tube with enzyme extract kept in dark would serve as blank, while the tube without extract but kept in light would serve as control. Activity of SOD is the difference in NBT reduction monitored at 560 nm in light with and without enzyme extract. One unit of activity is the amount of protein required to inhibit 50% initial reduction of NBT under light.

Catalase (CAT, E.C. 1.11.1.6)

Catalase activity was measured spectrophotometrically by following the oxidation of H_2O_2 at 240 nm according to the method of Patterson et al. (1984). The reaction mixture contained 50 mM sodium phosphate buffer (pH 7.0), 19 mM H_2O_2 and enzyme extract equivalent to 25 µg protein in a final volume of 3 ml. $\Delta\varepsilon$ for H_2O_2 at 240 nm was 43.6 mM^{-1} cm^{-1}.

Ascorbate peroxidase (APX, E.C. 1.11.1.11)

Ascorbate peroxidase activity was examined by the method of Nakano and Asada (1981). The reaction mixture for measuring APX activity contained 50 mM sodium phosphate buffer (pH 7.0), 0.2 mM EDTA, 0.5 mM ascorbic acid, 250 mM H_2O_2 and enzyme extract equivalent to 50 µg of protein. The activity was recorded as decrease in absorbance at 290 nm for 1 min and the amount of ascorbate oxidized was calculated from the extinction coefficient of 2.8 mM^{-1} cm^{-1}.

Glutathione reductase (GR, E.C. 1.6.4.2)

The activity of GR was determined by modifying the method of Jiang and Zhang (2001). The reaction mixture contained 25 mM sodium phosphate buffer pH 7.5, 10 mM GSSG, 3 mM $MgCl_2$ and 1 mM NADPH in a total volume of 2 ml. The reaction was started by addition of enzyme extract containing 50 µg protein and GR activity was monitored as NADPH oxidation ($\varepsilon = 6.2$ mM^{-1} cm^{-1}) by monitoring the decrease in absorbance at 340 nm.

Monodehydroascorbate reductase (MDAR, E.C. 1.6.5.4)

Monodehydroascorbate reductase activity was assayed by monitoring NADPH oxidation ($\varepsilon = 6.2$ mM^{-1} cm^{-1}) at 340 nm (Drazkiewicz et al. 2003). The reaction mixture (3 ml) contained 50 mM sodium phosphate buffer, pH 6.0, 2.5 mM ascorbic acid, 0.1 mM NADPH and enzyme extract equivalent to 100 µg of protein. The reaction was started by the addition of 4 units of ascorbate oxidase.

Activity staining of SOD

Native polyacrylamide gel electrophoresis (PAGE) was performed using the Laemmli (1970) buffer systems at 4°C for SOD. Samples were mixed with 10% glycerol (v/v) and 0.025% bromophenol blue before loading onto the gels. In each lane, enzyme extract containing 150 µg of protein was loaded. The gels were run at constant current of 100 V at 4°C in Amersham electrophoresis apparatus (Fairfield, CT, USA).

Isozymes of SOD were visualized according to Beauchamp and Fridovich (1971) as modified by Rucinska et al. (1999) in a 10% native gel with 10% glycerol in resolving as well as stacking gel at 4°C. SOD activity in the native gel was examined as the inhibition of NBT reduction by superoxide ion radicals generated photochemically. After electrophoresis, the gels were soaked in 2.45 mM NBT for 20 min, followed by incubation in a solution containing 50 mM potassium phosphate buffer (pH 7.8), 28 mM TEMED, 2.4 µM riboflavin under light until the SOD bands appear on a dark background. Different isoforms of SOD were identified by selective inhibition with H_2O_2 and potassium cyanide following the method of Salin and Bridges (1981). To inhibit the activity of Cu/Zn-SOD and Fe-SOD, gels were stained in the above buffer containing 5 mM H_2O_2. Selective inhibition of Cu/Zn-SOD was achieved by pre-incubating the gels in buffer containing 5 mM KCN. Densitometry of SOD bands was performed using Image J software 1.37 V, National Institute of Health, USA.

Estimation of ascorbate and dehydroascorbate

Ascorbate content was measured according to the method of Foyer et al. (1983). Aliquots of mesophyll protoplasts equivalent to 25 µg of chlorophyll in reaction medium (600 µl) were withdrawn at 0 min and after incubation for 10 min in dark or light (1,000 µmol m^{-2} s^{-1}) in the absence and presence of mitochondrial inhibitors. The reaction was stopped by adding ice-cold $HClO_4$ (final concentration 0.5 M) to the samples and the supernatant was collected for the analysis of Asc and DHA after centrifuging at 4°C for 10 min at 10,000*g*. The pH of the supernatant was increased approximately to 5.6 by stepwise addition of 1.25 M potassium carbonate. The precipitate formed was removed by centrifugation (10,000*g*, 6 min, 4°C) and supernatant was used for estimation of Asc, DHA and total ascorbate according to the methods described in Foyer et al. (1983).

Estimation of glutathione

After the treatment of mesophyll protoplasts with and without mitochondrial inhibitors at 0 min and after incubation for 10 min in dark or light (1,000 μmol m^{-2} s^{-1}), the reaction was stopped by adding 7% sulfosalicylic acid. The samples were centrifuged at 4,500*g* for 10 min and the supernatant was neutralized by the addition of 20 μl of 7.5 M triethanolamine. Total, oxidized, reduced glutathione were determined spectrophotometrically at 412 nm by the cycling method described by Griffith (1980). Total glutathione was determined by monitoring the changes in absorbance at 412 nm. The assay mixture (2 ml) contained 100 mM phosphate buffer (pH 7.5), 2 mM EDTA, 6.3 mM 5-5[1]-dithiobis-(2-nitrobenzoic acid), 5 mM NADPH, 1 unit of GR (from yeast, Boehringer Mannheim, Germany) and the neutralized protoplast extract (100 μl). All values are expressed as GSH (reduced form of glutathione) equivalents, determined from a GSH standard curve. For the estimation of GSSG (oxidized form of glutathione), 0.01 ml of 2-vinyl pyridine (2 V-P) was added to 0.5 ml of neutralized extract, so as to mask GSH and GSSG was extrapolated from a standard plot for GSSG. The solution was stirred for 1 min and incubated for 1 h at 25°C. Neutralized extraction medium served as a blank. Total glutathione was determined by reference to a standard curve of GSH and reduced glutathione was determined as the difference between the total glutathione and the oxidized form of glutathione.

Replications

The data presented are the average values of results (±SE) from four experiments conducted on different days. The differences between treatments were analyzed by one-way ANOVA, Student–Newman–Keuls method of multiple comparison analysis using SigmaStat 3.1 software (San Jose, CA, USA).

Results

Relation between photosynthetic carbon assimilation and ROS during restricted mitochondrial electron transport

The effect of mitochondrial inhibitors AA (inhibitor of COX pathway) or SHAM (inhibitor of AOX pathway) on photosynthetic carbon assimilation was examined by monitoring the changes in the steady-state rates of photosynthetic oxygen evolution in mesophyll protoplasts of pea at optimal CO_2 of 1.0 mM $NaHCO_3$ and saturating light intensity of 1,000 μmol m^{-2} s^{-1}. Both these compounds remarkably decreased the rates of photosynthetic oxygen evolution in mesophyll protoplasts by 50 and 44%, respectively (Fig. 1a). In controls, the steady-state rates (177 ± 7.7 μmol mg^{-1} chl h^{-1}) of photosynthetic O_2 evolution attained after a brief lag period of 3 min were stable over a time period of at least 20–30 min in retaining >90% of its activity (data not shown). However, so as to avoid errors due to perturbations in the stability of mesophyll protoplasts at room temperature, all treatments in the present study were restricted to a time period of 10 min under light. At the chosen concentrations of AA (0.1 μM) and SHAM (0.5 mM) where the effects on photosynthesis were significant, the total respiratory capacity of COX and AOX pathways of mesophyll protoplasts was affected only marginally by 18 and 20%, respectively (Fig. 1b).

In contrast to the effects on photosynthesis, there was a remarkable rise in intra-cellular ROS as measured by DCF fluorescence when the electron transport through COX pathway or AOX pathway is restricted under light. The relative units of DCF fluorescence increased by 1.86- and 3.22-fold over control (without inhibitor) after illuminating the mesophyll protoplasts for 10 min in the presence of AA and SHAM, respectively (Fig. 2). The ROS levels also increased under darkness, when the electron transport through COX or AOX pathway is restricted using AA or SHAM. However, the increase in ROS under darkness was not as significant as in light. The pronounced increase in the ROS levels of mesophyll protoplasts after illumination in the presence of AA and SHAM was also further confirmed by confocal microscopic studies (Fig. 3).

To critically evaluate the relationship between photosynthesis and cellular ROS, the rise in DCF fluorescence and the inhibition of photosynthesis were correlated in mesophyll protoplasts at a wide range of concentrations of AA (0–0.5 μM) and SHAM (0–1.0 mM) (Fig. 4a, b). SHAM has esterase-like activity and can directly enhance the DCF fluorescence (Hsiao and Bornman 1993). Similar to SHAM, AA also enhanced the DCF fluorescence in reaction medium used to illuminate mesophyll protoplasts. Hence, in the present study, we have taken care to plot the corrected values of DCF fluorescence (Supplementary Table 1) obtained by the reaction of H_2DCF with AA or SHAM in the absence of protoplasts in Figs. 2, 4a, b. The DCF fluorescence increased from 1.6 in control, i.e., without inhibitor to 9.9 and 13.2 in the presence of 0.5 μM AA and 1.0 mM SHAM, respectively. On the other hand, the photosynthesis decreased by 59 and 47% of control rates in the presence of these inhibitors (Fig. 4a, b).

The changes in D1 protein, an important component of PS II, were also examined in the presence of AA or SHAM to understand if the reduction in photosynthetic oxygen evolution or increase in cellular ROS caused any damage to D1 protein. In spite of the rise in intra-cellular ROS levels

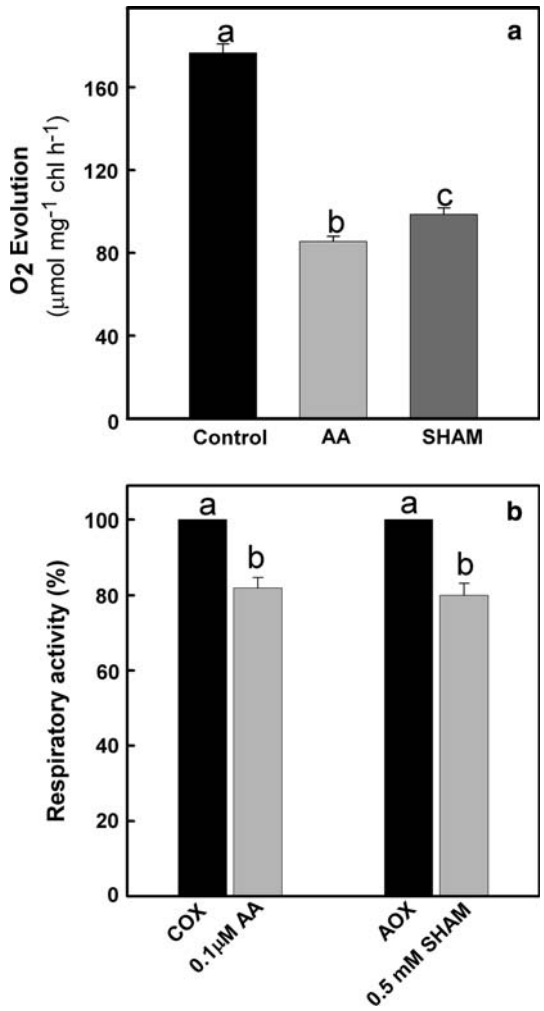

Fig. 1 **a** Effect of AA (0.1 μM) or SHAM (0.5 mM) on photosynthesis in mesophyll protoplasts of pea at optimal (1.0 mM $NaHCO_3$) CO_2 and saturating (1,000 μmol m^{-2} s^{-1}) light intensity. The rates of O_2 evolution were taken at steady-state photosynthesis (i.e., at the end of 10 min illumination), after a brief dark period of 5 min. **b** Effect of 0.1 μM AA or 0.5 mM SHAM on the capacity of COX pathway and AOX pathway. Total respiration, capacity of COX pathway and AOX pathways were 12.00 ± 0.68, 5.00 ± 0.79 and 4.47 ± 0.62 μmol O_2 uptake mg^{-1} chl h^{-1}, respectively, and were determined as described in "Materials and methods". Values represent the mean ± SE of four experiments. *Different letters* represent values that are statistically different (ANOVA test, $P \leq 0.05$)

and reduction in photosynthetic O_2 evolution, D1 protein levels were very stable even at concentrations as high as 1.0 μM AA or 5.0 mM SHAM (Fig. 4c, d). Both AA and SHAM did not have any affect on either photosynthesis or ROS levels in isolated chloroplasts (Table 1).

Effect of restricted mitochondrial electron transport on antioxidant enzymes in light

The observed perturbations in cellular ROS in the presence of AA or SHAM in light were further evaluated by

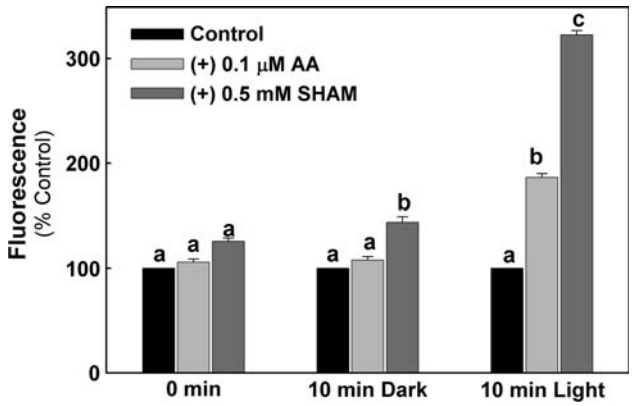

Fig. 2 Effect of AA (0.1 μM) or SHAM (0.5 mM) on intra-cellular ROS in pea mesophyll protoplasts at 0 min and after incubation for 10 min in dark or light (1,000 μmol m^{-2} s^{-1}) at optimal (1.0 mM $NaHCO_3$) CO_2. Steady-state ROS levels were assessed using the ROS-sensitive probe H_2DCF-DA as described in "Materials and methods". The relative DCF fluorescence min^{-1} in controls were 0.45 ± 0.06 (0 min), 0.90 ± 0.04 (10 min dark) and 1.6 ± 0.05 (10 min light). Values represent the mean ± SE of four experiments. *Different letters* represent values that are statistically different (ANOVA test, $P \leq 0.05$)

monitoring changes in the following antioxidant enzymes during steady-state photosynthesis: (a) SOD, scavenger of superoxide, (b) CAT and APX, scavengers of H_2O_2, and (c) MDAR and GR, important enzymes in regenerating Asc and GSH. Activity staining of native PAGE according to Salin and Bridges (1981) revealed the presence of one isoform related to each of Mn-SOD, Cu/Zn-SOD and Fe-SOD in mesophyll protoplasts of pea (Supplementary Fig. 1). The changes in the antioxidant enzymes showed similar trend in both dark and light after incubation for 10 min in the presence of AA or SHAM, compared with samples at 0 min (Figs. 5, 6). However, the changes were more pronounced in light, compared with treatments in dark. Treatment of mesophyll protoplasts with AA or SHAM showed increase in the activity of all the SOD isoforms related to three groups in native gels during steady-state photosynthesis (14–37% of control), compared with dark (10–20% of control) or treatment at 0 min (<4% of control) (Fig. 5a). Further, the increase in the total enzymatic activity of SOD as detected by spectrophotometric method in dark or light was more pronounced in the presence of SHAM (38 and 60% of control), compared with AA (20 and 38% of control), respectively (Fig. 5b).

The changes in total cellular activities of CAT in the presence of AA and SHAM were shown in Fig. 6a. Restriction of COX pathway had no effect on the activity of CAT in light, compared with dark (increased by 26% of control), while restriction of AOX pathway caused increase in the activity of CAT in dark (39% of control) as well as light (57% of control) (Fig. 6a). In contrast to other antioxidant enzymes, restriction of COX or AOX pathway had

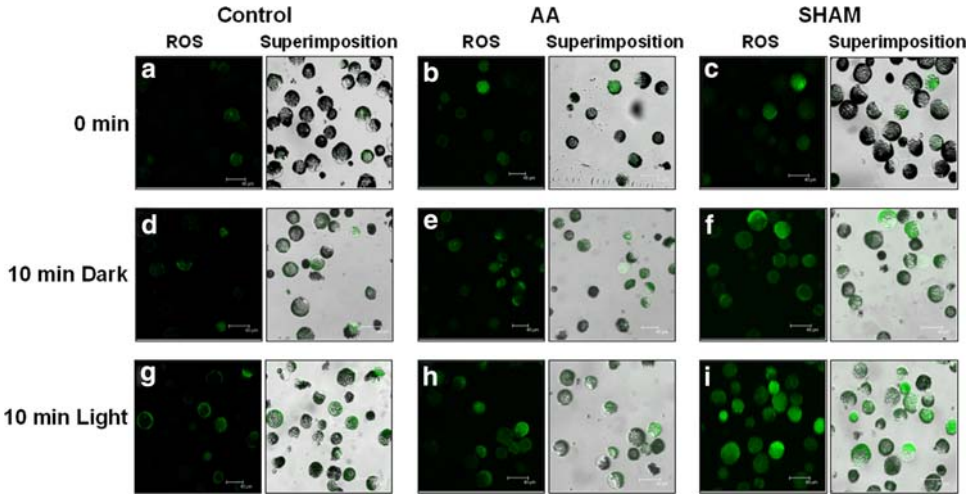

Fig. 3 Confocal fluorescence images of pea mesophyll protoplasts at 0 min and after incubation for 10 min in dark or light (1,000 μmol m^{-2} s^{-1}) at optimal (1.0 mM $NaHCO_3$) CO_2 with and without mitochondrial inhibitors. **a**, **b**, **c** DCF fluorescence images at 0 min without mitochondrial inhibitors (control) and with 0.1 μM AA or 0.5 mM SHAM, respectively. **d**, **e**, **f** DCF fluorescence images taken after dark without mitochondrial inhibitors (control) and with 0.1 μM AA or 0.5 mM SHAM, respectively. **g**, **h**, **i** DCF fluorescence images taken after light without mitochondrial inhibitors (control) and with 0.1 μM AA or 0.5 mM SHAM, respectively. Superimposition of the fluorescent and bright field images is also shown beside the fluorescence images for each treatment. These images are the representative of at least six independent experiments performed in different days

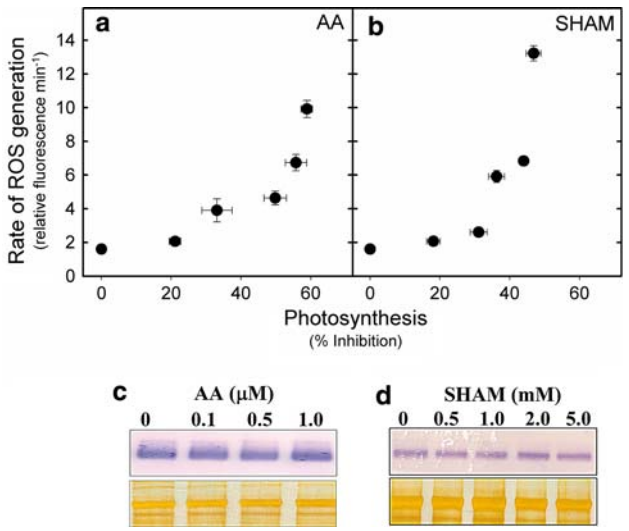

Fig. 4 Correlation between the relative rates of photosynthesis (as % inhibition of control) and rate of ROS generation in mesophyll protoplasts after incubation with AA or SHAM at optimal (1.0 mM $NaHCO_3$) CO_2 and saturating light intensity (1,000 μmol m^{-2} s^{-1}) for 10 min. These data are obtained with different concentrations of mitochondrial inhibitors: **a** 0–0.5 μM of AA; **b** 0–1.0 mM of SHAM as described elsewhere in text. Further details are as shown in Figs. 1 and 2 and as described in "Materials and methods". **c**, **d** Western blot analysis of D1 protein in mesophyll protoplasts treated with AA or SHAM. Mesophyll protoplasts illuminated for 10 min with different concentrations of AA and SHAM were homogenized in extraction buffer and the proteins (8 μg) were separated on SDS-PAGE. PVDF membrane with the transferred proteins was probed with antibodies raised against D1. Equal loading of protein was confirmed by silver staining of a duplicate gel. Representative results of four independent experiments are shown. Other details were as mentioned in "Materials and methods"

no effect on total cellular activity of APX neither in dark nor in light (Fig. 6b). However, restriction of COX pathway or AOX pathway caused significant increase in the total cellular activities of MDAR and GR in both dark and light (Fig. 6c, d). Irrespective of the dark or light treatment, the increase in the activities of MDAR and GR was more pronounced in the presence of AA (up to 49 and 65% of control rates), compared with SHAM (up to 43 and 55% of control rates), respectively (Fig. 6c, d).

Effect of restricted mitochondrial electron transport on antioxidant molecules in light

In plant cells, the major soluble small molecular weight antioxidant metabolites, Asc and GSH with their corresponding oxidized forms DHA and GSSG, function as efficient redox couples in maintaining cellular redox homeostasis and as secondary signals in ROS-mediated signal transduction pathways. The cellular Asc redox state is indicated by the Asc/DHA ratio, while the GSH redox state is indicated by the GSH/GSSG ratio. The changes in Asc, DHA, Asc plus DHA and redox ratio of Asc were more significant in light (51% of control), compared with changes in dark (<12% of control) (Fig. 7a–d). However, restriction of COX pathway or AOX pathway caused increase in ascorbate levels up to 14 and 66% of control (Fig. 7a). The total cellular DHA levels increased significantly by >1.8- and >5.8-fold of controls in dark and light, respectively, and the increase was more pronounced in the presence of SHAM when compared with AA (Fig. 7b).

Table 1 Effect of AA (0.1 μM) or SHAM (0.5 mM) on photosynthesis and ROS levels in isolated chloroplasts

Parameters	(−) inhibitor	(+) AA	(+) SHAM
Photosynthesis (μmol O_2 evolution mg^{-1} chl h^{-1})	53.9 ± 1.25	53.1 ± 2.06	51.84 ± 0.91
ROS (relative fluorescence min^{-1})	3.69 ± 0.12	3.74 ± 0.09	3.76 ± 0.18

Chloroplasts were incubated in dark for 5 min in reaction medium with or without (control) mitochondrial inhibitors before switching on light. Photosynthesis and ROS levels were determined at the end of 10 min illumination. Data represent mean ± SE ($n = 4$)

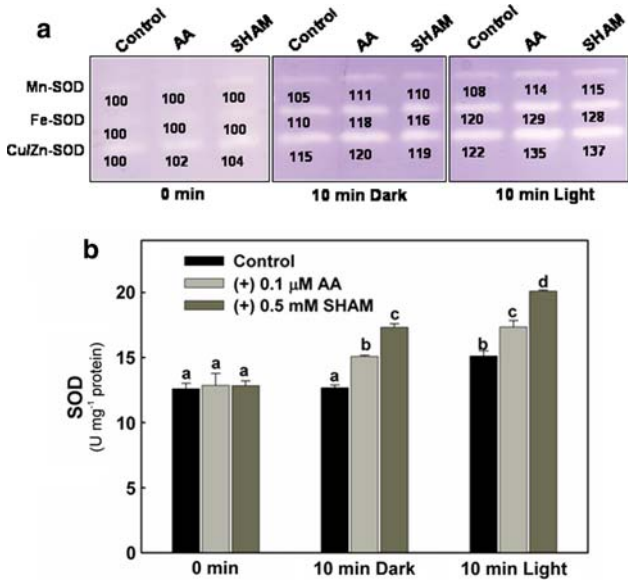

Fig. 5 Effect of AA or SHAM on the activity of SOD. **a** Activity staining of SOD as visualized on native PAGE. The changes in different SOD isoforms in mesophyll protoplasts were detected at 0 min and after incubation for 10 min in dark or light (1,000 μmol m^{-2} s^{-1}) at optimal (1.0 mM $NaHCO_3$) CO_2 without mitochondrial inhibitors (control) and with 0.1 μM AA or 0.5 mM SHAM. Densitometric values (as % of 0 min control) were indicated below the bands of each isoform of SOD. **b** Total cellular activity of SOD was determined by spectrophotometric method in mesophyll protoplasts at 0 min and after incubation for 10 min in dark or light (1,000 μmol m^{-2} s^{-1}) at optimal (1.0 mM $NaHCO_3$) CO_2, without and with 0.1 μM AA or 0.5 mM SHAM, respectively. Further details were as indicated in Fig. 1 and as described in "Materials and methods". Values represent the mean ± SE of four experiments. *Different letters* represent values that are statistically different (ANOVA test, $P \leq 0.05$)

While the total cellular levels of Asc plus DHA increased by >21% and ≥2.0-fold in dark and light, respectively, in the presence of AA or SHAM, compared with treatment at 0 min (Fig. 7c), the Asc redox state decreased from 8.4 to 6.5 (dark) and 3.4 (light) in the presence of AA and from 8.4 to 5.5 (dark) and 2.4 (light) in the presence of SHAM, respectively (Fig. 7d). This remarkable decrease in Asc redox ratio in light in the presence of SHAM is possibly due to the significant rise in cellular DHA levels (Fig. 7d).

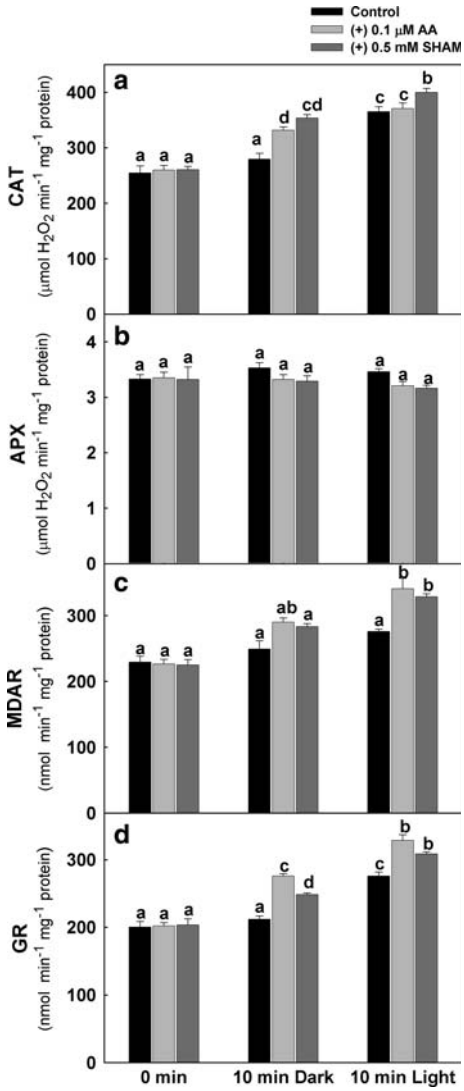

Fig. 6 Effect of AA or SHAM on the activity of CAT, APX, MDAR and GR. Total cellular activities of CAT (**a**), APX (**b**), MDAR (**c**) and GR (**d**) were determined by spectrophotometric method in mesophyll protoplasts at 0 min and after incubation for 10 min in dark or light (1,000 μmol m^{-2} s^{-1}) at optimal (1.0 mM $NaHCO_3$) CO_2, with and without 0.1 μM AA or 0.5 mM SHAM, respectively. Further details were as described in Fig. 1 and as described in "Materials and methods". Values represent the mean ± SE of four experiments. *Different letters* represent values that are statistically different (ANOVA test, $P \leq 0.05$)

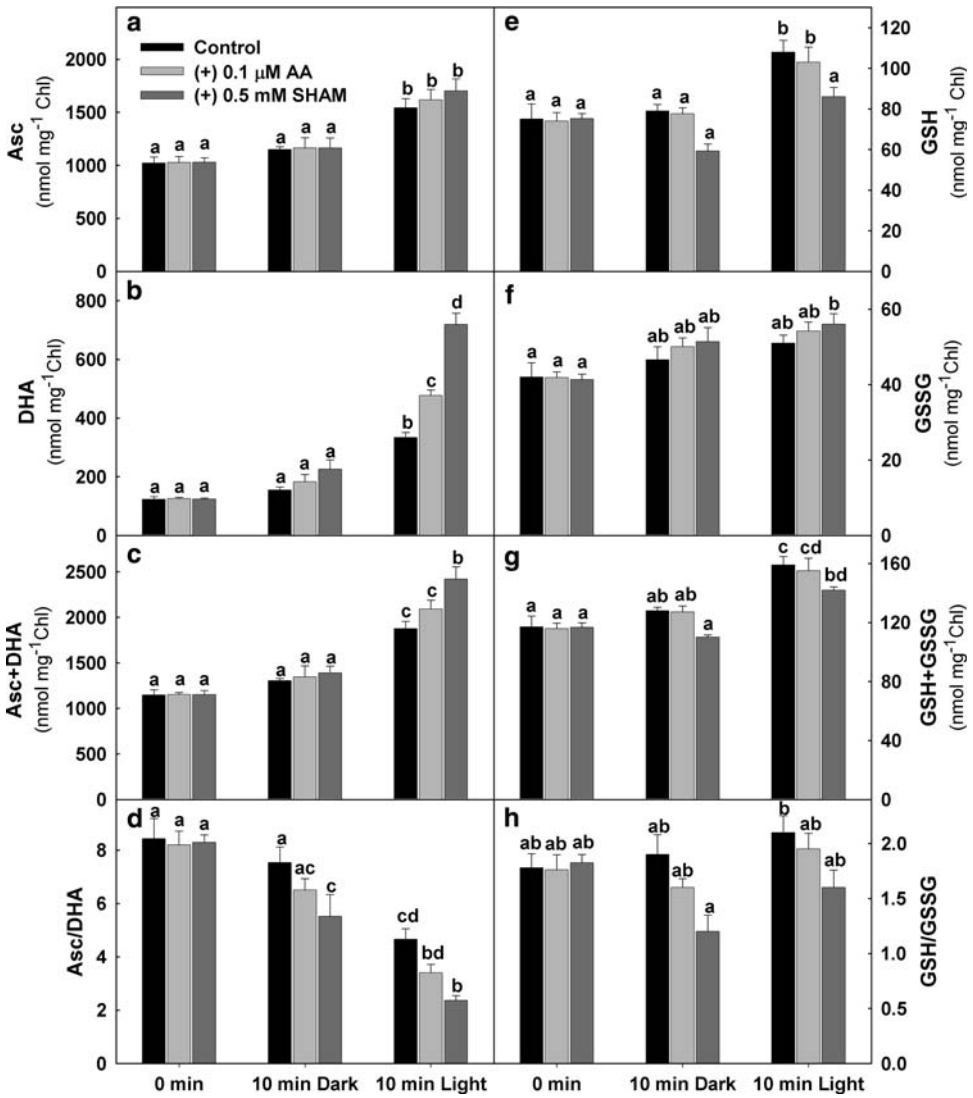

Fig. 7 Effect of AA and SHAM on the total cellular levels of Asc (**a**), DHA (**b**), Asc + DHA (**c**), Asc/DHA (**d**), GSH (**e**), GSSG (**f**), GSH + GSSG (**g**) and GSH/GSSG (**h**), in mesophyll protoplasts at 0 time and after incubation for 10 min in dark or light (1,000 μmol m^{-2} s^{-1}) at optimal (1.0 mM $NaHCO_3$) CO_2 without or with 0.1 μM AA and 0.5 mM SHAM, respectively. Further details were as described in Fig. 1 and "Materials and methods". Values represent the mean ± SE of four experiments. *Different letters* represent values that are statistically different (ANOVA test, $P \leq 0.05$)

Similar to changes in different components of Asc redox couple, the changes in the components of GSH redox couple—GSH, GSSG, GSH plus GSSG, redox ratios—were more prominent in light, compared with dark or treatments at 0 min (Fig. 7e–h). In contrast to Asc, GSH levels decreased in dark (from 105 to 79%) and light (from 144 to 114%), in the presence of both AA and SHAM, respectively, compared with treatments at 0 min (Fig. 7e). However, irrespective of the dark or light treatment, the decrease was more pronounced in the presence of SHAM compared with AA. Restriction of COX pathway or AOX pathway increased the GSSG levels marginally both in dark (from 112 to 121%) and light (from 121 to 133%), compared with treatments at 0 min (Fig. 7f). The total GSH plus GSSG levels also decreased marginally in dark (from 109 to 94%) and light (from 136 to 121%), compared with treatments at 0 min, in the presence of both AA and SHAM (Fig. 7g). Subsequently, the redox ratio of GSH also decreased from 1.9 to 1.6 (AA) and 1.2 (SHAM) in dark and from 2.1 to 1.9 (AA) and 1.6 (SHAM) in light, compared with treatments at 0 min (Fig. 7h).

Discussion

Mitochondrial oxidative metabolism modulates the coordination between different components of photosynthetic carbon assimilation in chloroplasts such as generation and use of assimilatory power (ATP and NADPH), induction of photosynthesis, maintenance of metabolites and the light activation of calvin cycle enzymes (Padmasree and Raghavendra 1999a, b, 2001a, b; Igamberdiev et al. 1998; Yoshida et al. 2006, 2007). In the present study, we focused on the changes in the patterns of cellular ROS, antioxidant enzymes and antioxidant molecules in response to light when electron transport through COX (or) AOX pathway of mitochondrial oxidative metabolism is restricted to reveal their importance during the beneficial

interactions of mitochondrial metabolism with photosynthetic carbon assimilation.

Use of metabolic inhibitors to examine the interactions between chloroplasts and mitochondria

In the present study, we used the metabolic inhibitors AA and SHAM which are easily permeable through the plasma membrane of protoplasts to restrict the flow of electrons through the COX and AOX pathways, respectively. The general perturbations caused to the metabolic system due to the non-specific effects of both AA and SHAM were minimized using these compounds at very low concentrations. Further at the chosen concentrations of AA (0.1 μM) and SHAM (0.5 mM), in spite of a marginal interference (<20%) in the respiratory capacity of COX and AOX pathways, there was a remarkable decrease (<50%) in the rates of photosynthetic oxygen evolution and significant increase (3.2-fold) in total cellular ROS of mesophyll protoplasts in light (Figs. 1a, b, 2). However, neither AA nor SHAM had any direct effect on the photosynthetic O_2 evolution rates or ROS levels in isolated chloroplasts (Table 1). Besides our own work with mesophyll protoplasts (Padmasree and Raghavendra 2001b), Yoshida et al. (2006) also indicated that AA at 0.1 μM concentration did not exert any large direct effects on cyclic electron transport of photosynthesis in leaves. While examining in detail the effects of 250 μM AA on photosynthesis, Takahashi et al. (2009) suggested that the inhibition of photosynthesis by AA is partly due to the interference of mitochondrial respiration. In the present study, we also evaluated the marginal interference in the respiratory capacity of COX pathway by 0.1 μM AA with changes in ATP/ADP ratios which were decreased by 30% in light when compared to their ratios in the absence of AA (data not shown).

ROS play an important role during the beneficial interactions between chloroplasts and mitochondria to optimize photosynthetic carbon assimilation

The strong positive correlation between the rise in total cellular levels of DCF fluorescence and inhibition of $NaHCO_3$-dependent O_2 evolution at a wide range of concentrations of both AA and SHAM demonstrates the importance of ROS during the beneficial interactions of mitochondrial electron transport with photosynthetic carbon assimilation (Fig. 4a, b). Any restriction in mitochondrial electron transport is known to cause over-reduction of respiratory complexes and generation of ROS in mitochondria (Møller 2001; Foyer and Noctor 2003; Navrot et al. 2007). Further, the following observations made through fluorimetric and confocal microscopy in the present study provided indirect evidences for the contribution of both mitochondria and chloroplast in rising the total cellular ROS in light: (a) pronounced increase in total cellular ROS in light when compared to darkness (Figs. 2, 3) and (b) negligible change in ROS levels in isolated illuminated chloroplasts (Table 1). The relative importance of AOX pathway over COX pathway in maintaining cellular ROS was shown with *A. thaliana* knock out mutants for AOX1a, which produced more ROS when compared to wild-type plants when treated with AA (Strodtkötter et al. 2009). H_2DCF-DA was used to analyze the changes in cellular H_2O_2 levels (Maxwell et al. 1999). Hence, we attribute the changes observed in ROS in the present study could be mostly due to H_2O_2 (Figs. 2, 3, 4a, b). The role of ROS as signal during the beneficial interactions between chloroplasts and mitochondria is further strengthened by the insignificant changes observed in D1 protein, which is known to be vulnerable to degradation by any increase in ROS levels (Fig. 4; Murata et al. 2007).

ROS mediates beneficial interactions between chloroplasts and mitochondria through changes in antioxidant enzymes

The perturbations in cellular ROS caused due to restriction in mitochondrial electron transport under steady-state photosynthesis were monitored by examining the changes in the activities of the following antioxidant enzymes which play a role in scavenging of ROS and regeneration of antioxidant metabolites related to Asc–GSH cycle: (a) SOD, (b) CAT, (c) APX, (d) MDAR and (e) GR (Noctor and Foyer 1998; Chew et al. 2003; Mittler et al. 2004; Amirsadeghi et al. 2006). The substantial increase in all the isoforms of SOD (chloroplastic, mitochondrial, peroxisomal and cytosolic) in the presence of AA and SHAM demonstrates the participation of antioxidant enzymes during the beneficial interactions between mitochondria and chloroplasts to optimize photosynthetic carbon assimilation (Fig. 5a). While the changes in the activities of SOD and CAT were more pronounced in the presence of SHAM, AA caused a notable increase in the activities of MDAR and GR during steady-state photosynthesis (Figs. 5b, 6a, c, d). In spite of the suggested sensitivity of APX to H_2O_2, we did not observe any such changes in its activity when electron transport through COX or AOX pathway is restricted in light (Fig. 6b; Miyake and Asada 1996).

ROS mediates beneficial interactions between chloroplasts and mitochondria through changes in antioxidant molecules

In plant cells, perturbations in the steady-state level of ROS are also detected through changes in cellular redox couples such as Asc/DHA and GSH/GSSG, which ultimately

require electrons from redox pairs such as NADPH/NADP (Foyer and Noctor 2003, 2005; Noctor 2006; Navrot et al. 2007). In *vtc* mutants which are deficient in biosynthesis of Asc, the sensitivity of leaf discs to undergo photoinhibition was enhanced in the presence of AA and SHAM (T. Sai Krishna et al., University of Hyderabad, personal communication). The significant decrease in redox ratio of Asc (indicated by Asc/DHA) in the presence of AA and SHAM suggests the importance of both COX and AOX pathways in maintaining cellular homeostasis buffered by Asc/DHA redox couple in light (Fig. 7d).

The ratios of GSH/GSSG were found to vary to changes in oxygen concentration in roots (6.1) and leaf cells (14.8) (Skutnik and Rychter 2009). However, such high redox ratios related to GSH were not observed in control samples in the present study. This could be attributed to the variation in the experimental material used or variation in technique used or variation in sample treatments applied to monitor the changes in different components of GSH redox couple. However, the observed decrease in the redox ratio of GSH (indicated by GSH/GSSG) under steady-state photosynthesis only in the presence of SHAM but not AA suggests the importance of AOX pathway in maintaining cellular homeostasis buffered by GSH/GSSG redox couple (Fig. 7h). In CAT-deficient mutant (*cat2*) of *Arabidopsis*, H_2O_2 induced accumulation of glutathione, indicating the importance of glutathione in maintaining cellular redox homeostasis (Queval et al. 2009). Unlike animal models, in plant cells, though the information on the direct role of reduced GSH in scavenging H_2O_2 is very limited, it plays a role in detoxification of H_2O_2 along with Asc through Asc–GSH cycle (Noctor and Foyer 1998). Nevertheless, several plant genes that showed homology to mammalian phospholipids hydroperoxide GSH peroxidase have been isolated recently (Rouhier et al. 2008).

Concluding remarks

The observations from the present study clearly indicate that any perturbation in the capacities of the COX or AOX pathway of mitochondrial oxidative electron transport in light leads to disturbances in the sustenance of photosynthesis through modulation in ROS, antioxidant enzymes and antioxidant molecules. However, it is intriguing to understand how the restriction in electron transport through COX pathway or AOX pathway of mitochondria in cellular environment is simultaneously coordinated with decline in chloroplastic photosynthesis through changes in ROS and different components of antioxidant system. More detailed studies involving transgenic and reverse genetics along with the holistic approach of systems biology are required to unravel the biochemical signals and molecular mechanisms underlying the beneficial interactions between chloroplasts and mitochondria to optimize photosynthetic carbon assimilation.

Acknowledgments This work was supported by grants to K.P.S. from Department of Science and Technology (No. SR/FTP/LS-226/2000). The support of funds to the Department of Plant Sciences and School of Life Sciences from DST-FIST level II (SR/FST/LSII-010/2007) and UGC-CAS-I (F-5-8/2008, SAP-II) is gratefully acknowledged. The authors are grateful to Dr. G. Padmaja, and CIL, UoHyd, for their help in statistical analysis and confocal microscopic studies. Ch.D. is a recipient of Senior Research Fellowship from Council of Scientific and Industrial Research. We thank Prof. Greg Vanlerberghe and Dr. T. Saradadevi for helpful discussion and suggestions related to the manuscript.

References

Amirsadeghi S, Robson CA, McDonald AE, Vanlerberghe GC (2006) Changes in plant mitochondrial electron transport alter cellular levels of reactive oxygen species and susceptibility to cell death signaling molecules. Plant Cell Physiol 47:1509–1519

Apel K, Hirt H (2004) Reactive oxygen species: metabolism, oxidative stress, and signal transduction. Annu Rev Plant Biol 55:373–399

Asada K (1999) The water–water cycle in chloroplasts: scavenging of active oxygen and dissipation of excess photons. Annu Rev Plant Physiol Plant Mol Biol 50:601–639

Bartoli CG, Yu J, Gomez F, Fernandez L, McIntosh L, Foyer CH (2006) Inter-relationships between light and respiration in the control of ascorbic acid synthesis and accumulation in *Arabidopsis thaliana* leaves. J Exp Bot 57:1621–1631

Beauchamp C, Fridovich I (1971) Superoxide dismutase: improved assays and an assay applicable to acrylamide gels. Anal Biochem 44:276–287

Carrari F, Nunes-Nesi A, Gibon Y, Lytovchenko A, Ehlers-Loureiro M, Fernie AR (2003) Reduced expression of aconitase results in an enhanced rate of photosynthesis and marked shifts in carbon partitioning in illuminated leaves of wild species tomato. Plant Physiol 133:1322–1335

Chew O, Whelan J, Millar AH (2003) Molecular definition of the ascorbate-glutathione cycle in *Arabidopsis* mitochondria reveals dual targeting of antioxidant defenses in plants. J Biol Chem 278:46869–46877

del Rio LA, Sandalio LM, Corpas FJ, Palma JM, Barroso JB (2006) Reactive oxygen species and reactive nitrogen species in peroxisomes: production, scavenging and role in cell signaling. Plant Physiol 141:330–335

Doulis AG, Debian N, Kingston-Smith AH, Foyer CH (1997) Differential localization of antioxidants in maize leaves. Plant Physiol 114:1031–1037

Drazkiewicz M, Skorzynska-Polit E, Krupa Z (2003) Response of ascorbate-glutathione cycle to excess copper in *Arabidopsis thaliana* (L.). Plant Sci 164:195–202

Dutilleul C, Driscoll S, Cornic G, De Paepe R, Foyer CH, Noctor G (2003) Functional mitochondrial complex I is required by tobacco leaves for optimal photosynthetic performance in photorespiratory conditions and during transients. Plant Physiol 131:264–275

Fiorani F, Umbach AL, Siedow JN (2005) The alternative oxidase of plant mitochondria is involved in the acclimation of shoot growth at low temperature. A study of Arabidopsis *AOX1a* transgenic plants. Plant Physiol 139:1795–1805

Foyer CH, Noctor G (2003) Redox sensing and signaling associated with reactive oxygen in chloroplasts, peroxisomes and mitochondria. Physiol Plant 119:355–364

Foyer CH, Noctor G (2005) Oxidant and antioxidant signaling in plants: a re-evaluation of the concept of oxidative stress in a physiological context. Plant Cell Environ 28:1056–1071

Foyer CH, Rowell J, Walker D (1983) Measurement of the ascorbate content of spinach leaf protoplasts and chloroplasts during illumination. Planta 157:239–244

Gardeström P, Igamberdiev AU, Raghavendra AS (2002) Mitochondrial functions in light. In: Foyer CH, Noctor G (eds) Photosynthetic nitrogen assimilation and associated carbon and respiratory metabolism. Kluwer Academic Publishers, The Netherlands, pp 151–172

Graham D (1980) Effects of light on dark respiration. In: Davies DD (ed) The biochemistry of plants: a comprehensive treatise. Academic Press, New York, pp 525–579

Griffith OW (1980) Determination of glutathione and glutathione disulfide using glutathione reductase and 2-vinyl-pyridine. Anal Biochem 106:207–212

Hoefnagel MHN, Atkin OK, Wiskich JT (1998) Interdependence between chloroplasts and mitochondria in the light and the dark. Biochim Biophys Acta 1366:235–255

Hsiao KC, Bornman CH (1993) Salicylhydroxamic acid mimics esterase-like action. J Exp Bot 44:1847–1849

Igamberdiev AU, Hurry V, Krömer S, Gardeström P (1998) The role of mitochondrial electron transport during photosynthetic induction. A study with barley (*Hordeum vulgare*) protoplasts incubated with rotenone and oligomycin. Physiol Plant 104:431–439

Jiang M, Zhang J (2001) Effect of abscissic acid on active oxygen species, antioxidative defense system and oxidative damage in leaves of maize seedlings. Plant Cell Physiol 42:1265–1273

Krömer S (1995) Respiration during photosynthesis. Annu Rev Plant Physiol Plant Mol Biol 46:45–70

Krömer S, Stitt M, Heldt HW (1988) Mitochondrial oxidative phosphorylation participating in photosynthetic metabolism of a leaf cell. FEBS Lett 226:352–356

Krömer S, Malmberg G, Gardeström P (1993) Mitochondrial contribution to photosynthetic metabolism. A study with barley (*Hordeum vulgare*) leaf protoplasts at different light intensities and CO_2 concentrations. Plant Physiol 102:947–955

Kuzniak E, Sklodowska M (2005) Compartment-specific role of the ascorbate-glutathione cycle in the response of tomato leaf cells to *Botrytis cinerea* infection. J Exp Bot 56:921–933

Laemmli UK (1970) Cleavage of structural proteins during the assembly of the head of bacteriophage T4. Nature 227:680–685

Lowry OH, Rosebrough NJ, Farr AL, Randall RJ (1951) Protein measurement with the folin phenol reagent. J Biol Chem 193:265–275

Maxwell DP, Wang Y, McIntosh L (1999) The alternative oxidase lowers mitochondrial reactive oxygen production in plant cells. Proc Natl Acad Sci USA 96:8271–8276

Mittler R, Vanderauwera S, Gollery M, Breusegem FV (2004) Reactive oxygen gene network of plants. Trends Plant Sci 9:490–498

Miyake C, Asada K (1996) Inactivation mechanism of ascorbate peroxidase at low concentration of ascorbate; hydrogen peroxide decomposes compound I of ascorbate peroxidase. Plant Cell Physiol 37:423–430

Møller IM (2001) Plant mitochondria and oxidative stress: electron transport, NADPH turnover, and metabolism of reactive oxygen species. Annu Rev Plant Physiol Plant Mol Biol 52:561–591

Møller IM, Jensen PE, Hansson A (2007) Oxidative modifications to cellular components in plants. Annu Rev Plant Biol 58:459–481

Murata N, Takahashi S, Nishiyama Y, Allakhverdiev SI (2007) Photoinhibition of photosystem II under environmental stress. Biochim Biophys Acta 1767:414–421

Nakano Y, Asada K (1981) Hydrogen peroxide is scavenged by ascorbate-specific peroxidase in spinach chloroplasts. Plant Cell Physiol 22:867–880

Navrot N, Rouhier N, Gelhaye E, Jacquot JE (2007) Reactive oxygen species generation and antioxidant systems in plant mitochondria. Physiol Plant 129:185–195

Noctor G (2006) Metabolic signaling in defence and stress: the central roles of soluble redox couples. Plant Cell Environ 29:409–425

Noctor G, Foyer CH (1998) Ascorbate and glutathione: keeping active oxygen under control. Annu Rev Plant Physiol Plant Mol Biol 49:249–279

Noctor G, De Paepe R, Foyer CH (2007) Mitochondrial redox biology and homeostasis in plants. Trends Plant Sci 12:125–134

Noguchi K, Yoshida K (2008) Interaction between photosynthesis and respiration in illuminated leaves. Mitochondrion 8:87–99

Nunes-Nesi A, Carrari F, Lytovchenko A, Smith AMO, Loureiro ME, Ratcliffe RG, Sweetlove LJ, Fernie AR (2005) Enhanced photosynthetic performance and growth as a consequence of decreasing mitochondrial malate dehydrogenase activity in transgenic tomato plants. Plant Physiol 137:611–622

Nunes-Nesi A, Sulpice R, Gibon Y, Fernie AR (2008) The enigmatic contribution of mitochondrial function in photosynthesis. J Exp Bot 59:1675–1684

Padmasree K, Raghavendra AS (1999a) Importance of oxidative electron transport over oxidative phosphorylation in optimizing photosynthesis in mesophyll protoplasts of pea (*Pisum sativum* L.). Physiol Plant 105:546–553

Padmasree K, Raghavendra AS (1999b) Response of photosynthetic carbon assimilation in mesophyll protoplasts to restriction on mitochondrial oxidative metabolism: metabolites related to the redox status and sucrose biosynthesis. Photosynth Res 62:231–239

Padmasree K, Raghavendra AS (2001a) Consequence of restricted mitochondrial oxidative metabolism on photosynthetic carbon assimilation in mesophyll protoplasts: decrease in light activation for four chloroplastic enzymes. Physiol Plant 112:582–588

Padmasree K, Raghavendra AS (2001b) Restriction of mitochondrial oxidative metabolism leads to suppression of photosynthetic carbon assimilation but not of photochemical electron transport in pea mesophyll protoplasts. Curr Sci 81:680–684

Padmasree K, Padmavathi L, Raghavendra AS (2002) Essentiality of mitochondrial oxidative metabolism for photosynthesis: optimization of carbon assimilation and protection against photoinhibition. Crit Rev Biochem Mol Biol 37:71–119

Palma JM, Jiminez A, Sandalio LM, Corpas FJ, Lundqvist M, Gomez M, Sevilla F, del Rio LA (2006) Antioxidative enzymes from chloroplasts, mitochondria, and peroxisomes during leaf senescence of nodulated pea plants. J Exp Bot 57:1747–1758

Patterson BD, Payne LA, Chen Y, Graham D (1984) An inhibitor of catalase induced by cold chilling-sensitive plants. Plant Physiol 76:1014–1018

Queval G, Thominet D, Vanacker H, Miginiac-Maslow M, Gakière B, Noctor G (2009) H_2O_2 activated up-regulation of glutathione in *Arabidopsis* involves induction of genes encoding enzymes involved in cysteine synthesis in the chloroplast. Mol Plant 2:344–356

Raghavendra AS, Padmasree K (2003) Beneficial interactions of mitochondrial metabolism with photosynthetic carbon assimilation. Trends Plant Sci 8:546–553

Raghavendra AS, Padmasree K, Saradadevi K (1994) Interdependence of photosynthesis and respiration in plant cells: interactions between chloroplasts and mitochondria. Plant Sci 97:1–14

Rouhier N, Lemaire SD, Jacquot JP (2008) The role of glutathione in photosynthetic organisms: emerging functions for glutaredoxins and glutathionylation. Annu Rev Plant Biol 59:143–166

Rucinska R, Waplak S, Gwozdz E (1999) Free radical formation and activity of antioxidant enzymes in lupin roots exposed to lead. Plant Physiol Biochem 37:187–194

Salin ML, Bridges SM (1981) Absence of iron-containing superoxide dismutase in mitochondria from mustard (*Brassica campestris*). Biochem J 195:229–233

Skutnik M, Rychter AM (2009) Differential response of antioxidant systems in leaves and roots of barley subjected to anoxia and post-anoxia. J Plant Physiol 116:926–937

Strodtkötter I, Padmasree K, Dinakar CH, Speth B, Niazi PS, Wojtera J, Voss I, Do PT, Nunes-Nesi A, Fernie AR, Linke V, Raghavendra AS, Scheibe R (2009) Induction of the AOX1D isoform of alternative oxidase in *A. thaliana* T-DNA insertion lines lacking isoform AOX 1A is insufficient to optimize photosynthesis when treated with AA. Mol Plant 2:284–297

Sundar D, Perianayaguy B, Reddy AR (2004) Localization of antioxidant enzymes in the cellular compartments of sorghum leaves. Plant Growth Regul 44:157–163

Sweetlove LJ, Lytovchenko A, Morgan M, Nunes-Nesi A, Taylor NL, Baxter CJ, Eickmeier I, Fernie AR (2006) Mitochondrial uncoupling protein is required for efficient photosynthesis. Proc Natl Acad Sci USA 103:19587–19592

Takahashi S, Milward SE, Fan DY, Chow WS, Badger MR (2009) How does cyclic electron flow alleviate photoinhibition in Arabidopsis. Plant Physiol 149:1560–1567

Towbin H, Staehlin T, Gordon J (1979) Electrophoretic transfer of proteins from polyacrylamide gels to nitrocellulose sheets. Procedure and some applications. Proc Natl Acad Sci USA 76:4350–4354

Vanlerberghe GC, Robson CA, Yip JYH (2002) Induction of mitochondrial alternative oxidase in response to a cell signal pathway down-regulating the cytochrome pathway prevents programmed cell death. Plant Physiol 129:1829–1842

Watanabe CK, Hachiya T, Terashima I, Noguchi K (2008) The lack of alternative oxidase at low temperature leads to a disruption of the balance in carbon and nitrogen metabolism, and to an up-regulation of antioxidant defence systems in *Arabidopsis thaliana* leaves. Plant Cell Environ 31:1190–1202

Yoshida K, Terashima I, Noguchi K (2006) Distinct roles of the cytochrome pathway and alternative oxidase in leaf photosynthesis. Plant Cell Physiol 47:22–31

Yoshida K, Terashima I, Noguchi K (2007) Up-regulation of mitochondrial alternative oxidase concomitant with chloroplast over-reduction by excess light. Plant Cell Physiol 48:606–614